View metadata, citation and similar papers at core.ac.uk
brought to you by CORE
provided by NASA Technical Reports Server

Modeling Strategies for Superconducting Microstrip Transmission Line Structures

Kongpop U-Yen, Karwan Rostem, and Edward J. Wollack, *Senior Member, IEEE*

***Abstract*—Strategies are explored to reduce the electromagnetic simulation time of electrically large superconducting transmission line structures while retaining model accuracy. The complex surface reactance of an infinite thin-film superconducting sheet is evaluated with the BCS (Bardeen-Cooper-Schrieffer) theory and used as an input to model the phase velocity and characteristic impedance of finite width transmission line structures. Commercially available electromagnetic simulation software are employed for the calculations and the results are compared with limiting analytic forms from the literature. The influences of line width, metallization thickness, and substrate height on microstrip transmission line propagation are considered in detail and a scaling approach is presented to compensate for the leading order effect in numerical simulations. These findings are particularly important near the energy gap of the superconductor due to the influence of the kinetic inductance on the transmission line dispersion.**

***Index Terms*—Electromagnetic propagation, Finite Element Analysis, Method of Moments, Microstrip transmission lines, Superconductors.**

I. Introduction

PLANAR superconducting microstrip transmission lines have been widely used in cryogenic microwave and millimeter-wave systems. Over typical frequency and parameter ranges of interest these low-loss thin-film structures can be realized with a well defined impedance, have a quasi-TEM symmetry, and approximate single-mode propagation [1], [2]. The range of applicability for these desirable characteristics is limited by the finite binding energy of electron (Cooper) pairs in the thin film metallization [3], losses in the dielectric substrate, and the onset of higher order propagating modes and radiation to free-space arising from the finite substrate thickness relative to the radiation wavelength [4].

Given a detailed knowledge of material properties, the microstrip transmission line geometry can be used to suitably define and control the impedance scale and signal propagation. Characteristic impedance levels in microstrip transmission lines from a few to $\approx 100\,\Omega$ are readily achievable and enable compact planar transmission line structures. When used in conjunction with its complementary slotline, co-planar waveguide, or parallel plate waveguide structures, these transmission line elements provide a rich pallet for the synthesis and realization of superconducting electronic circuitry.

To realize these functions the propagation characteristics of transmission line structures must be adequately controlled. In microstrip, tolerances are primarily a function of the line width, height, and substrate permittivity [5]. The thickness of the line [6] and ground planes, surface finish of metallization layers, and homogeneity of dielectrics [7] typically play secondary roles. The enclosure geometry, inter-line spacing, spurious radiation excitation [1], and onset of surface wave propagation [4] also present practical considerations in defining the isolation between planar structures and the overall fidelity of the packaged system response. The introduction of superconducting elements in the architecture also necessitates consideration of the metallization purity, grain structure, and uniformity, as well as, the details of the end operational environment.

For structures involving superconducting elements, an accurate representation of the dynamic or kinetic inductance associated with Cooper pairs is needed to achieve a high fidelity representation of the circuit response in electromagnetic (EM) simulations. This is a widely explored practical problem [8], [9], [10] and in the limiting case of a simple microstrip line, analytical solutions for the characteristic impedance and effective phase velocity have been derived using conformal mapping [11]. The Wheeler incremental inductance rule [12], [13] provides an analytically trackable means of computing the complex surface impedance when the line dimensions and radius of curvature are much greater than the depth of field penetration. This perturbative approach provides significant physical insight, however, has not lead to a general treatment of edge and junction effects present in planar geometries. Homogenous dielectrics with rectangular conductors [14] and associated ground plane losses [15] represent other extensions and limiting cases of interest. Alternatively, equivalent boundary condition approaches for modeling of superconducting transmission line structures can be employed in numerical simulations [16].

In general, a three dimensional representation of circuit elements and fields in an EM simulator is needed to accurately predict the transmission line propagation properties. However, this can be computationally challenging for relatively simple transmission line structures with high aspect ratios or large electrical lengths, especially when an accurate representation of the phase delay is a driving performance consideration in the design. This has lead to the representation of superconducting layers using a surface impedance approximation for zero thickness (ZT) trace and ground metallization layers

Kongpop U-yen is with the NASA/GSFC, Greenbelt, MD 20771 USA (email: kongpop.u-yen-1@ nasa.gov).

Karwan Rostem is with the Johns Hopkins University, Baltimore, MD 21287 USA (email: Karwan.rostem@nasa.gov).

Edward J. Wollack is with the NASA/GSFC, Greenbelt, MD 20771 USA (email: edward.j.wollack@ nasa.gov).

This work was supported in part by the National Aeronautics and Space Administration (NASA) Astrophysics Research and Analysis (APRA) and the Goddard Space Flight Center (GSFC) Internal Research and Development (IRAD) programs.

in transmission line model simulations [8], [9]. From this perspective, models of finite thickness (FT) structures can be constructed from sheets appropriately interconnected with edge metallization sheets or vias and simulated with significantly reduced computational resources.

In this work, scaling considerations are reviewed and presented in Section II, which provide a path to address the challenges in efficiently modeling superconducting structures of finite width with high fidelity. In Section III, the details of the model geometry and electromagnetic finite element simulations (FEM) performed are presented. In Section IV, the results of finite- and zero-thickness microstrip transmission line models are presented and the scaling relationships between these solutions are evaluated. Finally in Section V, the accuracy and applicability of this general approach are discussed in the context of a representative five-section transmission line filter simulation.

II. Electromagnetic Considerations

The surface impedance of a superconducting media of infinite lateral extent having metallization thickness, t, and London penetration depth, λ_L, can be expressed as,

$$Z_s = j\omega\mu_o\lambda_L \coth(t/\lambda_L), \tag{1}$$

where ω and μ_o are the angular frequency and free-space permeability [3], [16]. This reduces to the commonly used formula, $Z_s \simeq j\omega\mu_o\lambda_L$, in the bulk limit, $t \gg \lambda_L$. In the finite thickness limit a transmission line model can be used to compute the effective sheet impedance for a superconducting trace excited on one side. The resulting impedance can be expressed as a product of separable functions,

$$Z_s^{FT}(t/h, t/\lambda_L) = \zeta(t/\lambda_L) \cdot Z_s(t/\lambda_L), \tag{2}$$

where ζ accounts for the magnetic energy stored in the superconducting media (see Ref. [8], Fig. 6),

$$\zeta \cong \left[1 - \frac{t/\lambda_L}{2\coth(t/\lambda_L)} + \sqrt{1 + \left(\frac{t/\lambda_L}{2\coth(t/\lambda_L)}\right)^2}\right]. \tag{3}$$

Equation 2 approximates the characteristic impedance, Z_o, of microstrip lines to 4% relative to analytical results for trace-width to substrate-height ratios, $w/h < 7$ [11].

Inspired by the success of this method for infinite superconducting layers with finite metallization thickness, generalization of the method to accommodate the influence of the finite line width is advocated through the use of effective propagation parameters. Implementing the microstrip trace and ground plane layers as zero-thickness structures, a separable function, ξ, is numerically evaluated while enforcing the following relationship:

$$Z_s^{ZT}(w/h, t/h, t/\lambda_L) = \xi(w/h, t/h) \cdot Z_s^{FT}(t/h, t/\lambda_L). \tag{4}$$

In this approach the scaling function, ξ, maps effects of crowding of the current density for a strip of finite width, w, and thickness, t, onto an equivalent zero-thickness trace. Forcing the phase velocity, $v_{phase} = 1/\sqrt{\mu_{eff} \cdot \epsilon_{eff}}$, of microstrip lines with finite trace dimensions to be equivalent to a zero-thickness structure can reduce the size of a computational problem. In self-consistently carrying out this phase velocity matching procedure it is useful to recall that the media's wave impedance, $Z_{wave} = \sqrt{\mu_{eff}/\epsilon_{eff}}$, is also linked to the effective permittivity, ϵ_{eff} and permeability, μ_{eff} of the transmission line [10]. This allows a unique specification of wave propagation on the equivalent transmission line system. While this method is inherently applicable to two dimensional transmission line structures in the mean field approximation, no attempt has been made to correct for junction effects between abutted line sections with differing effective surface impedances.

The physical energy densities of the field configuration remains integrable and finite over the entire domain defined by the model. For the case of conducting surfaces, the singular components of the electric and magnetic field vectors scale inversely with the square root of the distance from the edge, while the field strengths parallel to the edge component are finite [17]. These effects increase the energy density near the metallization edges [14], [18] and the resulting change in propagation properties can be seen as a direct result of minimizing the free energy associated with the current distribution across the transmission line structure geometry in the presence of kinetic inductance.

III. Electromagnetic Simulations

The functional decomposition proposed in Eq. 4 is explored for uniform microstrip lines. The microstrip lines are represented as either perfect electric conductor or niobium superconducting films. In exploring this approach, the method of moments and finite-element EM solvers are used to numerically evaluate the scaling function, ξ. ANSYS HFSS is used as the base line electromagnetic simulator as it allows the non-linear frequency dependent thin-film properties of a superconductor to be fully implemented. The software capabilities are summarized in Table I.

TABLE I: EM solver package capabilities. ω_o is a constant reference frequency.

	HFSS v17.1	*Sonnet* v11.56	*Designer* v17.1 PlanarEM
Method	3D FEM	3D MoM	2D MoM
Simulation volume boundary	PEC	PEC	Radiation
EM port type	Full-Wave	Lumped	Lumped
Metallization thickness	Finite	Finite	Zero
Surface impedance, Z_s	$\omega\, L(\omega)$	$\omega\, L(\omega_o)$	$\omega_o\, L(\omega_o)$
2D scale function, ξ	Relative to 3D HFSS model	Relative to 3D *Sonnet* model	Relative to 3D HFSS model evaluated at ω_o

A. Microstrip Transmission Line Model

A microstrip transmission line with a 6 μm line width, w, and a 5 μm thick Si substrate, h, is used as a reference model. See Fig. 1 for the model configuration. A constant

and lossless relative dielectric function, ϵ_r =11.55, is adopted for simplicity to represent a cryogenic mono-crystalline bulk silicon substrate. A perfect electric conductor (PEC) is used as an enclosure above the line and along the walls of the microstrip to define a boxed configuration. See Table I for details of the model setup defined within each simulator package. The box width, W, is 60 μm and the box lid is 45 μm above the microstrip transmission line trace. A perfect magnetic wall was used to reduce the model size by enforcing a symmetry plane at the center of the microstrip line.

For simulating the finite-thickness microstrip, a kinetic inductance surface reactance is applied to all sides of the conductor and the inner volume is perfect electric conductor to eliminate the volume internal to the conductor in the model. The conductor thickness used in this paper is $t_1 = 0.29\,\mu$m and $t_2 = 0.25\,\mu$m for the microstrip and ground layers respectively, which reflect practical geometries implemented using micro-fabrication processes.

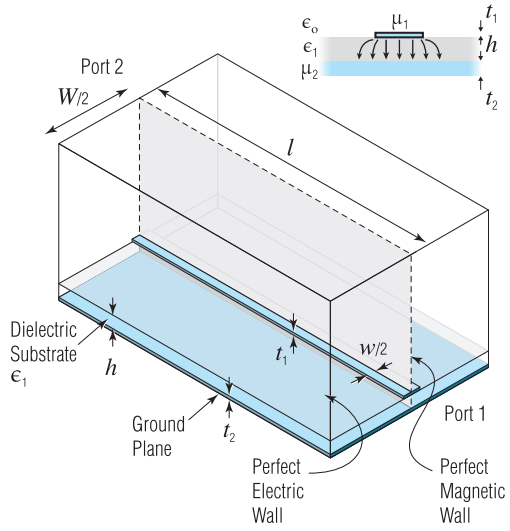

Fig. 1: Model of a boxed microstrip line and the boundary conditions used to validate HFSS and *Sonnet* simulations. A magnetic symmetry plane is used to reduce the model size. For *Designer*, the material layers are infinite in extent and the simulation boundaries provide an ideal termination.

B. Superconducting Metallization Specification

In addition to $\lambda_L(0)$ being a material dependent parameter, the associated change in the penetration length scale with frequency increases the challenge in modeling of the behavior of circuit elements. Arguably, accurately capturing the functional form of $\lambda_L(\omega)$ is essential to predicting the response of complex superconducting circuits. To specify the film properties, the kinetic sheet inductance as a function of frequency was evaluated using BCS theory [19] and applied to the ground and trace conductor surfaces. The computed sheet kinetic inductance, $L(\omega) = \mu_0\lambda_L(\omega)$, for Nb is shown in Fig. 2. A superconducting transition temperature, T_c of 9.2 K, and a zero temperature λ_L of 90 nm is adopted for Nb. The finite metallization thickness correction term, ζ, is computed and applied to the microstrip line surfaces following [8].

The kinetic inductance was applied as a frequency-dependent sheet reactance in HFSS through a polynomial curve fitting function. The kinetic inductance was introduced in the models as a surface reactance following Fig. 2 [8]. In *Sonnet*, a specific value is discretely applied at each simulation frequency. The response of the microstrip lines are evaluated between 10 and 450 GHz. This data is used to numerically verify that the line impedance and phase velocity follow the separation of frequency and spatial dependent variables specified in Eq. 4. The microstrip line parameters derived from evaluating this family of models are summarized in Table II. The EM simulations for this test case reveal that employing finite thickness Nb in HFSS provides the closest agreement to closed-form expressions for microstrip [2], while more significant deviations are observed when modeling a zero thickness Nb microstrip in HFSS, *Sonnet* or *Designer*. It is evident from this example that some form of compensation is needed to capture the propagation properties response with the desired fidelity.

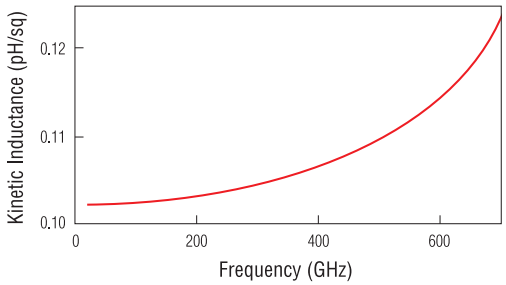

Fig. 2: Kinetic sheet inductance of a Nb film as a function of frequency for superconducting microstrip line derived from BCS theory [19].

TABLE II: Modeled microstrip line characteristics (90 GHz)

Approach	Trace Material	Ground Material	Z_o (Ω)	Phase Velocity (10^8 m/s)
Analytical [2]	ZT PEC	ZT PEC	41.9	1.078
HFSS	ZT PEC	ZT PEC	41.3	1.044
HFSS	FT PEC	ZT PEC	41.8	1.083
Sonnet	ZT PEC	ZT PEC	42.2	1.079
Designer	ZT PEC	ZT PEC	44.1	1.077
Analytical [5]	FT Nb	ZT Nb	41.2	1.038
HFSS	ZT Nb	ZT Nb	43.4	1.018
HFSS	FT Nb	ZT Nb	41.8	1.044
Sonnet	ZT Nb	ZT Nb	43.6	1.045
Designer	ZT Nb	ZT Nb	45.5	1.058

IV. Zero-Thickness Film Model Scaling Function

While the finite thickness surface reactance model can capture the propagation properties of the superconducting microstrip line structure, the computation time can be significantly higher and even prohibitive when modeling complex

circuit structures. To overcome this potential obstacle, Eq. 4 was used to evaluate the scaling function ξ from HFSS EM simulations, which maps the impedance and phase velocity of a finite thickness microstrip line onto a zero thickness film.

The scaling function is evaluated in two limiting cases. First, both the superconducting trace and ground layers of the microstrip are compensated with the same ξ value to produce an equivalent response to a microstrip line using a finite thickness film model. In another scenario, only the superconducting trace layer is compensated and the ground layer is modeled as a zero thickness perfect electric conductor. Microstrip with Si substrate thicknesses of 0.45, 1.5, and 5 μm were modeled with a line widths ranging from 2 μm to 24 μm. The scaling function, ξ, is determined by requiring the zero and finite thickness line models to yield the same phase velocity between 10 and 450 GHz with a fractional uncertainty less than $\pm 1\%$ under a matched port impedance termination.

The simulation results demonstrate the phase velocity correction, ξ, can be approximated as a linear function of the logarithm of the line-width to substrate dielectric thickness ratio. See dashed line in Fig. 3. When the kinetic inductance properties are only applied to the microstrip trace and the ground plane is treated as PEC, further reduction in model size can be achieved, however, the functional complexity of the phase velocity correction ξ increases. See solid line in Fig. 3 and note a break point in ξ is present near $w/h \simeq 2$. This corresponds to a transition in field confinement from being under the trace to less tightly bound in this region. From a circuit perspective this corresponds to the change in the characteristic impedance scale from low-to-high on the microstrip line [2]. In HFSS, less than a 6% difference in the characteristic impedance was observed over the range of zero and finite thickness models explored here.

The microstrip line configurations were also solved in two other EM software packages, *Designer* and *Sonnet*, to evaluate the characteristics of ξ via a methods of moment simulation approach. A similar functional form for ξ to that observed with HFSS is obtained using the method of moment analysis by *Sonnet*, see Fig. 4. In *Designer*, the kinetic inductance is applied as a constant surface impedance and for the 2D microstrip line structure, a reference frequency of 100 GHz is adopted.

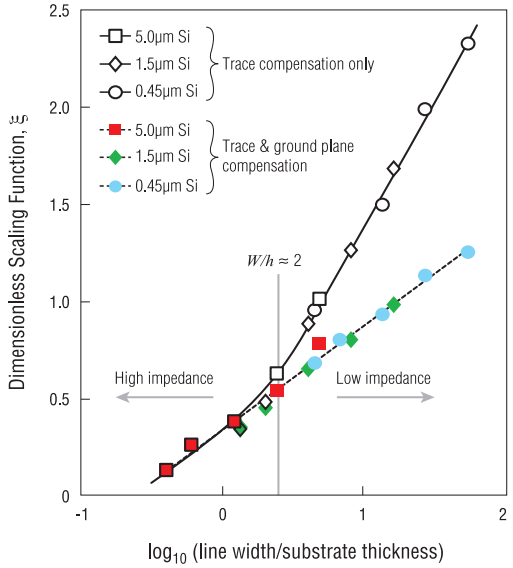

Fig. 3: Dimensionless scaling function, ξ, for microstrip as a function of line width over substrate thickness (HFSS: Si substrate $t_1 = 0.29\,\mu$m, $\epsilon_r = 11.55$). Data is presented for two cases: trace and ground plane layer compensation (dashed line) and trace compensation with a PEC ground plane (solid line). A breakpoint in the function ξ occurs in the second case near $w/h \simeq 2$, where the field confinement transitions from being largely under the trace to less tightly bound to the line.

V. Microstrip Filter Simulation

To quantify the validity and accuracy of the zero thickness scaling function in a representative application, the baseline S-parameter responses of a superconducting Nb microstrip transmission line filter with zero and finite thickness boundary conditions are calculated with HFSS. See Fig. 5 (top) for the microstrip filter's layout. Without correction, the zero thickness model produces $\sim$4% shift in the 3dB corner frequency compared to a finite thickness model. See middle panel in Fig. 5. To correct for this systematic deviation, the appropriate scaling function, ξ, is applied to the zero thickness superconducting film layer. The magnitude of the scaling function, ξ, was evaluated for each microstrip line width as dictated by the relationship derived from Fig. 3. The modeled

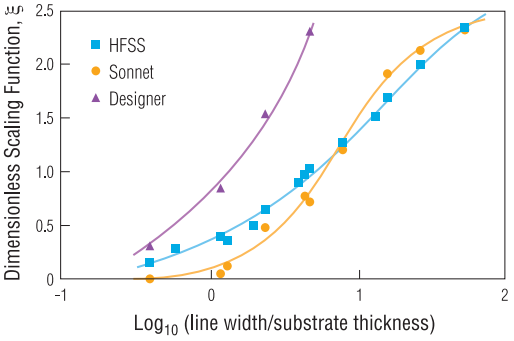

Fig. 4: Dimensionless scaling function, ξ, for microstrip as a function of line width over substrate thickness derived from *Designer* and *Sonnet* (Si substrate $t_1 = 0.29\,\mu$m, $\epsilon_r = 11.55$). Data is shown for microstrip trace compensation with a PEC ground plane. HFSS simulation results are also plotted for ease of comparison.

S-parameter response using a zero thickness film and ξ are in agreement with the finite thickness model. The observed shift in the filter's 3 dB corner frequency is less than 1%. In addition to tests performed in HFSS, the zero thickness scaling function approach was validated in *Sonnet* and *Designer*. The corresponding ξ value was evaluated for each microstrip line and applied to the trace layer while the ground plane remains a PEC.

The simulation results (Fig. 5; lower panel) show that the simulation in *Sonnet* produces similar S-parameter responses to that observed in HFSS, while the filter response in *Designer* remains relatively accurate in the vicinity of the reference frequency of 80 GHz where each ξ was evaluated and gracefully degrades with increasing spectral offset. This limitation could be addressed by varying the reference frequency, ω_o, for each simulation frequency of interest. See Table III for a summary of HFSS simulation durations. The *Sonnet* and *Designer* models are zero thickness and their simulation times are 23:15 and 3:01 (minute:second) respectively and independent of the use of the scaling function. One observes the model with finite thickness films essentially doubles the processing time required relative to the zero thickness model.

TABLE III: HFSS simulation time of the band-stop filter geometry specified in Figure 5. The S-parameter convergence, ΔS, value is achieved within the indicated simulation time. Simulations were carried out on a computer with Intel Xeon E5-1650 processor, 64 GByte of memory, and multi-processing feature enabled for eight CPU cores.

Conductor Material	Convergence Criteria, ΔS	Simulation time (minute:second)
2D PEC	0.018	19:44
2D Nb Uncompensated	0.016	30:01
2D Nb Compensated	0.012	37:19
3D Nb	0.014	50:40

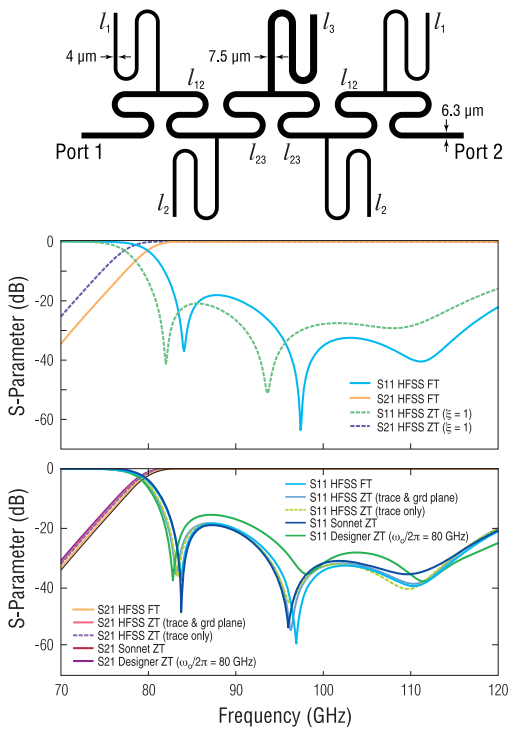

Fig. 5: (Top) Transmission line filter realized on 5 μm-thick silicon substrate used to validate the superconducting scaling model. The filter stub lengths ($l_1 = 499$, $l_2 = 457$, and $l_3 = 459\,\mu$m) and inter-section delay line ($l_{12} = 298$ and $l_{23} = 282\ \mu$m) are indicated. The structure's overall dimensions are 620 μm $\times$ 415 μm. (Middle) Simulations of niobium superconducting microstrip lines with finite and zero thickness models implemented in HFSS. Without compensation, the lower edge of the filter is shifted by ≈ 3 GHz or a fractional error ≈ 0.03, which represents a significant design bias in the realization of superconducting filters. (Bottom) Comparison of the compensation factor method performed with selected electromagnetic simulation tools. For *Designer* notice the superconductor's surface reactance is a constant set by the 80 GHz reference frequency.

VI. Conclusion

A zero-thickness sheet kinetic inductance scaling function is proposed to reduce EM simulation time for complex superconducting microwave circuits while maintaining comparable accuracy to results obtained with models containing finite-thickness films. Strategies for implementing the zero-thickness scaling function in three commonly employed EM simulation software packages were presented, however, this technique is broadly applicable to other EM numerical modeling tools. Variations on this theme are applicable to modeling other single-mode superconducting transmission line topologies. Experience suggests that the strategy retains utility in the limit the inter-line couplings represent a perturbation on the dominant mode of propagation. The accuracy of the numerical approach enables reliable design of superconducting filters for bolometric passband definition in broadband ground-based millimeter wave astronomical polarimetry and related applications. Improvements over the results described can be achieved thru refinement of the underlying convergence parameters employed in defining and extracting the transmission line scaling function.

References

[1] R. K. Hoffmann, "Handbook of Microwave Integrated Circuits," 1987, Artech House, Norwood MA, pp. 135.

[2] D. M. Pozar, "Transmission Lines and Waveguides," 2005, in Microwave Engineering, 3rd Ed. John Wiley & Sons, Hoboken NJ, ch. 3 sec. 3.8.

[3] M. Tinkham, "Introduction to Superconductivity," 1996, McGraw-Hill, pp. 68-71.

[4] K. Chang, "Handbook of Microwave and Optical Components," 1989, John Wiley & Sons, New York.

[5] R. Garg, "The effect of tolerances on microstripline and slotline performances," *IEEE Transactions on Microwave Theory and Techniques*, vol. 26, no. 1, pp. 16–19, Jan 1978.

[6] M. A. R. Gunston and J. R. Weale, "Variation of microstrip impedance with strip thickness," *Electronics Letters*, vol. 5, no. 26, pp. 697–698, December 1969.

[7] K.C. Gupta and R. Garg and I.J. Bahl, "Microstrip Lines and Slotlines," 1979, Artech House, Norwood MA, chapter 6.

[8] A. R. Kerr, "Surface Impedance of Superconductors and Normal Conductors in EM Simulators," 1999, MMA Memo No.245 - NRAO Electronics Division Internal Report No. 302.

[9] V. Belitsky, C. Risacher, M. Pantaleev, and V. Vassilev, "Superconducting microstrip line model studies at millimetre and sub-millimetre waves," *International Journal of Infrared and Millimeter Waves*, vol. 27, no. 6, pp. 809–834, 2006.

[10] G. Cataldo, E. J. Wollack, E. M. Barrentine, A. D. Brown, S. H. Moseley, and K. U-Yen, "Analysis and calibration techniques for superconducting resonators," *Review of Scientific Instruments*, vol. 86, no. 1, p. 013103, 2015.

[11] G. Yassin and S. Withington, "Electromagnetic models for superconducting millimetre-wave and sub-millimetre-wave microstrip transmission lines," *Journal of Physics D: Applied Physics*, vol. 28, no. 9, p. 1983, 1995.

[12] H. A. Wheeler, "Formulas for the skin effect," *Proceedings of the IRE*, vol. 30, no. 9, pp. 412–424, Sept 1942.

[13] H.-F. Huang and J.-F. Mao, "The inductance model of coupled high-tc superconducting microstrip lines," *IEEE Transactions on Applied Superconductivity*, vol. 14, no. 1, pp. 7–12, March 2004.

[14] D. M. Sheen, S. M. Ali, D. E. Oates, R. S. Withers, and J. A. Kong, "Current distribution, resistance, and inductance for superconducting strip transmission lines," *IEEE Transactions on Applied Superconductivity*, vol. 1, no. 2, pp. 108–115, June 1991.

[15] C. L. Holloway and G. A. Hufford, "Internal inductance and conductor loss associated with the ground plane of a microstrip line," *IEEE Transactions on Electromagnetic Compatibility*, vol. 39, no. 2, pp. 73–78, May 1997.

[16] Z.-Y. Shen, "High-Temperature Superconducting Microwave Circuits," 1994, Artech House, Norwood MA, pp. 81-86.

[17] J. Meixner, "The behavior of electromagnetic fields at edges," *IEEE Transactions on Antennas and Propagation*, vol. 20, no. 4, pp. 442–446, Jul 1972.

[18] R.F. Harrington, "Field Computation by Moment Methods," 1992, IEEE Press Series on Electromagnetic Waves, Piscataway, NJ, pp. 22-28.

[19] D. C. Mattis and J. Bardeen, "Theory of the anomalous skin effect in normal and superconducting metals," *Phys. Rev.*, vol. 111, pp. 412–417, Jul 1958. [Online]. Available: https://link.aps.org/doi/10.1103/PhysRev.111.412